Journal of Materials Chemistry B

Accepted Manuscript



This is an *Accepted Manuscript*, which has been through the Royal Society of Chemistry peer review process and has been accepted for publication.

Accepted Manuscripts are published online shortly after acceptance, before technical editing, formatting and proof reading. Using this free service, authors can make their results available to the community, in citable form, before we publish the edited article. We will replace this Accepted Manuscript with the edited and formatted Advance Article as soon as it is available.

You can find more information about *Accepted Manuscripts* in the **Information for Authors**.

Please note that technical editing may introduce minor changes to the text and/or graphics, which may alter content. The journal's standard <u>Terms & Conditions</u> and the <u>Ethical guidelines</u> still apply. In no event shall the Royal Society of Chemistry be held responsible for any errors or omissions in this *Accepted Manuscript* or any consequences arising from the use of any information it contains.



Journal of Materials Chemistry B

RSCPublishing

COMMUNICATION

One-Step Synthesis of Silver Nanoshell with Bumps for Highly Sensitive Near-IR SERS Nanoprobes†

Cite this: DOI: 10.1039/x0xx00000x

Homan Kang,‡a Jin-Kyoung Yang,b Mi Suk Noh,cde Ahla Jo,f Sinyoung Jeong,g Minwoo Lee,g Somin Lee,ch Hyejin Chang,g Hyunmi Lee,b Su-Ji Jeon,i Hye-In Kim,i Myung-Haing Cho,cd,h,j Ho-Young Lee,f* Jong-Ho Kim,i* Dae Hong Jeong,g* and Yoon-Sik Leea,b*

Received 00th January 2012, Accepted 00th January 2012

DOI: 10.1039/x0xx00000x

www.rsc.org/MaterialsB

A seedless, one-step synthetic route to uniform bumpy silver nanoshells (AgNS) as highly NIR sensitive SERS substrates is reported; these subtrates can incorporate Raman label compounds and biocompatible polymers on the their surface. AgNS based NIR-SERS probes are successfully applied to cell tracking in a live animal using a portable Raman system.

Since surface-enhanced Raman scattering (SERS)-based nanoprobes were first developed for biological applications, they have become an alternative to fluorescence-based labels in the fields of molecular detection, diagnosis, and bioimaging.^{1,2,3} SERS-based approaches for target detection and bio-imaging have many advantages, including excellent sensitivity affording single-molecular level multiplexing capability, 5,6,7 and resistance to photobleaching.8 For the sensitive detection of target molecules utilizing the advantages of SERS spectroscopy, SERS-active nanoparticles (NPs) such as nanoshells, 9,10,11 nanorods, 12 nanostars, 7,13 cluster/assembly-based NPs, 14,15,16 and bimetallic NPs, 17 which induce strong electromagnetic field enhancement, are essential. In particular, for successful applications of SERS technology in in vivo detection and imaging, not only must the SERS probes be effectively excited inside the deep tissues of living animals, but their signals must also be detected from outside of the tissue. In this regard, it is very important to tune the surface plasmonic resonance (SPR) of nanostructures toward the near-infrared (NIR) spectral region, so-called biological window (700-900 where tissue components show much lower absorption.^{3,15,18,19,20,21} Therefore, a strategy to design NIRsensitive plasmonic nanostructures which are able to maximize the enhancement of SERS signals under NIR excitation light remains crucial for practical in vivo applications of SERS technologies.

Metal nanoshells (NSs) composed of a dielectric core and a metal nanoshell are of great interest due to their tunable surface plasmon resonance (SPR) band from the visible to the IR region by modifying their core size, shell thickness, and atomic composition. Among the various metal NSs, silver and gold NSs have been considered as proper SERS-active substrates for the sensitive detection of target molecules due to the

considerable amplification of Raman signals by the strong electromagnetic field. 11,24 In particular, silver exhibits 10 to 1000-fold greater Raman enhancement than gold, 25 and has a higher tendency to form rough surface morphologies than gold in nanoshell formation.²⁶ Previously, several synthetic methods for the fabrication of silver NS (AgNS), including a multi-step layer-by-layer deposition, ^{27,28,29} a seed-mediated growth process, ^{23,24,26,30,31,32} and a sonochemical deposition process, ³³ have been reported. However, the previous approaches have not been satisfactory for an effective synthesis of a shell possessing the desired optical properties with its surface completely covered with pure silver. 23,24,26,28,30,31,33,34,35 In addition, these methods involve time-consuming multi-step processes and it is difficult to control the shell thickness for tuning the SPR band. Hence, for *in vivo* application and quantification, it is necessary to develop a simple, reproducible, and thickness-controllable approach for the effective synthesis of AgNS exhibiting NIR plasmonic absorption. In addition, the deposition of rough silver shells in which stronger near-field enhancement in the vicinity of the metal surface can be induced is more desirable than that of smooth silver shells for sensitive detection with SERS.11,27,36

Here, we report a reproducible and seedless, one-step synthetic route to a uniform bumpy silver nanoshell (AgNS) which can be a NIR sensitive SERS substrate. On the surface of the AgNS, Raman label compounds (RLCs) and biocompatible polymers can be incorporated. This approach allows an easy synthesis of a completely covered AgNS with bump-structures on its surface; it also enables the controllability of shell thickness in a one-step growth process. We demonstrate that the bumpy AgNS can serve as a highly sensitive and biocompatible NIR SERS probe. The bumpy AgNS coded with a simple aromatic compound, 4fluorobenzenthiol, was sensitive enough to detect Raman signals at a single-particle level (SERS enhancement factor: 6.4 $\times 10^{5}$) under NIR excitation (785 nm), which might be attributed to a strong electromagnetic field in the vicinity of the bumpy structures on the AgNS surface. In vivo toxicity of AgNS-based NIR-SERS probes (dose=50 mg kg⁻¹) was examined in a live animal, where results show no significant toxicity and side effect. The NIR-SERS probes were also examined using NIR SERS spectroscopy for their effective tracking of cells in a

60 70 50

COMMUNICATION

living animal. The results herein suggest that the bumpy AgNS based NIR-SERS probes can potentially be used for multiplex in vivo molecular detection and bio-imaging applications.

a) One-Step Bumpy Nanoshell Formation AgNO₃, octylamine in ethylene glycol 1h, Room temperature Bumpy Ag nanoshell (AgNS) Proposed Shell Growth Process Continuous & Fast growth e-based reduction process

Fig. 1 Synthesis and characterization of bumpy Ag nanoshell (AgNS). a) Schematic illustration of a seedless and one-step synthesis of complete AgNS with bumpstructures on its surface via reduction of Ag+ by octhylamine in ethylene glycol solution. b) Representative SEM image of bumpy AgNS at low magnification, and c) at high magnification, showing narrow size distribution and bump-structures on the surface. d) XRD pattern of bumpy AgNS showing metallic Ag with a facecentered-cubic (fcc) phase.

The synthetic scheme for bump-structured AgNS as a SERS substrate is shown in Fig. 1a. For the seedless and one-step fabrication of AgNS with a uniform bumpy surface, thiolfunctionalized silica nanospheres (ca. 150 nm in diameter) were used as a dielectric core. The thiol functional group plays a crucial role in the complete and uniform formation of AgNS on the silica surface due to the high affinity of thiol group with silver. Bumpy AgNS were then synthesized via the direct and fast reduction of a silver precursor (AgNO₃) on the silica surface in the presence of octylamine without deposition of seed metals. In this process, octylamine was used as a reducing agent³⁷ as well as a capping ligand,³⁸ which plays an important role for the fast formation of the silver shell under a mild condition (1h, room temperature) and for the control of its morphology and coverage on the silica surface.³⁹ Silver ions (Ag⁺) can be readily reduced by octylamine via a single electron transfer from an amino group in a symmetric diol solution (ethylene glycol), which leads to the nucleation of Ag⁰ in the vicinity of the silica surface to form a silver shell on the silica surface. The fast reduction kinetics of Ag+ at room temperature might be attributed to an increase in the reduction potential of Ag+ by creating an Ag+/symmetric diol chelate, compared to that of Ag⁺/ethanol chelate (cyclic voltammetry data is shown in ESI Fig. S1†).40 This increased reduction potential of Ag⁺ ions enables them to be effectively reduced by octylamine at room temperature, which leads to the facile formation of the silver shell for a short period of time. However, in the absence of octylamine, the silver shell did not form on the silica surface. In addition, when ethylene glycol monoethyl ether or ethanol was used as a medium instead of ethylene glycol, AgNS did not form on the silica surface at room temperature, as shown in ESI Fig. S2[†]. This result clearly

indicates that the monohydroxyl group could not chelate Ag+ ions as effectively as the symmetric diol.

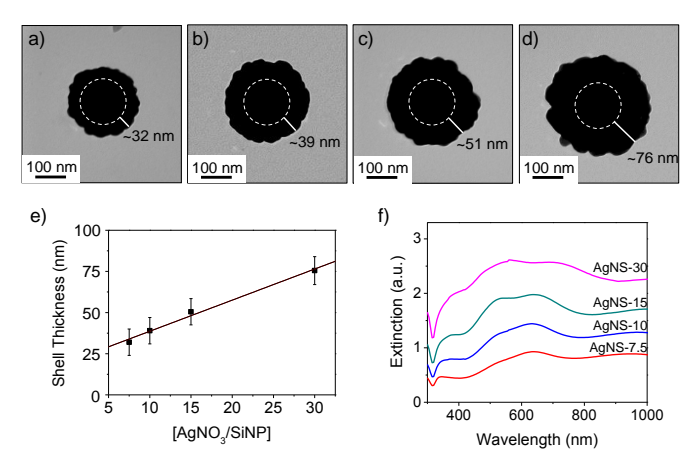


Fig. 2 Control of silver shell thickness of bumpy AgNS and its extinction spectra. TEM images of AgNS obtained at a weight ratio [AgNO₃/SiNP] of a) 7.5, b) 10, c) 15, and d) 30. The white dotted circles indicate a silica nanosphere core (~150 nm in diameter). The silver shell thickness increased gradually from ~32 nm to ~76 nm. e) Strong linear relationship between shell thickness and weight ratio [AgNO₃/SiNP] (r^2 =0.984) (mean \pm S.D., n = 30). f) Extinction spectra of bumpy AgNS. The numbers in the acronym AgNS indicate the weight ratio, [AgNO₃/SiNP], during synthesis.

The typical scanning electron microscopy (SEM) images of the AgNSs (prepared from 1 mg of thiol-functionalized silica nanospheres, 3.5 mM of AgNO₃, and 5 mM of octylamine) are shown in Figs. 1b and 1c. The low magnification of SEM image shows that the size of AgNS is uniform (301 \pm 17 nm, n = 30) and a portion of the incompletely covered AgNS was less than 1% (counted from ca. 400 AgNSs). According to the elemental mapping with energy dispersive X-ray spectroscopy (EDX), only a silver atom was observed in case there was no silicon atom for a core silica particle (ESI Fig. S3†), indicating that the thick silver shell fully covers the silica surface without any vacant sites. As shown in Fig. 1c, it is interesting that, without post-treatment such as extra deposition or chemical etching process, 36,41 the surface topography of AgNS has bumpy structures of 20-30 nm size rather than a smooth surface. This bumpy surface can induce stronger local electromagnetic field enhancement than a smooth surface, and is necessary for a strong SERS signal. 11,27,34 The typical X-ray diffraction (XRD) pattern of the bumpy AgNS is shown in Fig. 1d. The sharp diffraction peaks corresponding to the metallic silver with a face-centered-cubic (fcc) phase suggests the formation of highly crystalline silver.31

Next, we attempted to determine whether this seedless, one-step method could tune the thickness of the silver shell. The weight ratio of AgNO₃ to silica nanospheres (SiNP) [AgNO₃/SiNP] in solution was varied from 7.5 to 30 by decreasing the amount of SiNP. For the expression of the weight ratio of each sample, the AgNS synthesized at a weight ratio of 7.5, for example, was denoted as AgNS-7.5, in which the number indicates the weight ratio. Transmission electron microscopy (TEM) images of AgNS obtained from each reaction condition are shown in Figs. 2a-2d. The thickness of the silver shell gradually increased from ~32 nm (AgNS-7.5) to ~76 nm (AgNS-30) with an increase in the weight ratio of AgNO3 to SiNP. The shell thickness and the weight ratio of AgNO3 to SiNP showed a good linear relationship (r^2 =0.984) (Fig. 2e), suggesting that the thickness of the silver shell can be precisely controlled in this

Journal Name

synthesis (details of the size and thickness of AgNS are shown in ESI Table S1†). It should be noted that the surface topography of AgNS remains bumpy, regardless of the silver shell thickness (see ESI Fig. S4†), indicating that octylamine might act as a capping agent to protect the bump structures. The plasmonic extinction spectra of AgNS are shown in Fig. 2f. All AgNSs exhibit broad extinction bands from the visible to the NIR region (560 nm - 1000 nm). The large extension of the plasmonic extinction bands of AgNS is attributed to the shell and bumpy structure. The broad absorption feature of AgNS from the visible region to the NIR region is beneficial to the effective excitation of AgNS by NIR incident light.

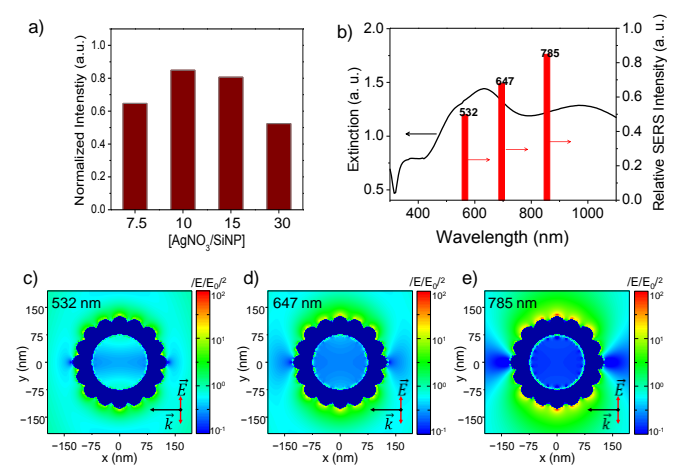


Fig. 3 SERS effect and E-field distribution of bumpy AgNS. a) Normalized SERS intensity of the peak at 1075 cm⁻¹ for 4-fluorobenzenethiol (4-FBT) adsorbed on four types of AgNSs dispersion prepared at different weight ratios [AgNO₃/SiNP] from 7.5 to 30. SERS intensities were normalized by the Raman intensity of the ethanol peak at 882 cm⁻¹. b) Relative SERS intensity of the peak at 1075 cm⁻¹ for 4-FBT on AgNS-10 under different excitation laser lines (532, 647, and 785 nm). Calculated E-field distributions of bumpy AgNS-10 under c) 532, d) 647, and e) 785 nm excitation laser lines using discrete dipole approximation (DDA). The nanoshells have a 27 nm inner shell thickness, a 204 nm diameter, and a 150 nm diameter silica core. The outer bump-nanostructures were assumed to have half sphere structures with a 21 nm radii.

To evaluate the SERS activity in the NIR window, we then conducted SERS measurements on bumpy AgNSs of different thicknesses (AgNS-7.5, 10, 15, and 30). After the 4fluorobenzenethiol (4-FBT) as a Raman label compound (RLC) was adsorbed on the surface of AgNSs, the SERS intensity of the 4-FBT Raman band at 1075 cm⁻¹ was measured by NIR laser excitation (785 nm). As shown in Fig. 3a, AgNS-10 with a shell thickness of ~39-nm exhibited the strongest SERS intensity under NIR laser excitation. To support these experimental results, the electric field (E-field) enhancements on the bumpy AgNS of different thicknesses were calculated using the discrete dipole approximation (DDA) at $\lambda = 785$ nm (see ESI Fig. S5†). The dimensions of bumpy AgNSs were determined based on electron microscope images. The simulation results revealed that the local field enhancement value in bumpy AgNS-10 was highest and 1.5 times higher than that in AgNS-30, which are consistent with the results of SERS measurements. In order to obtain further insights on the SERS effect of AgNS as a function of excitation wavelength, laser lights with three different wavelengths (532, 647, and 785 nm) were irradiated to AgNS-10. Bumpy AgNS-10 generates SERS signals of 4-FBT for all the laser-lines, as can be anticipated from its broad extinction band (Fig. 3b). However, the strongest

SERS intensity was obtained by NIR excitation at 785 nm, which is 1.7 times larger than that by the visible excitation at 532 nm. In order to understand the optical features of broad excitation in SERS, and the wavelength dependency on incident light from the visible to the NIR range, the E-field enhancements on the bumpy AgNS were calculated using the DDA at three different excitation laser lines of 532, 647, and 785 nm (Figs. 3c, 3d, and 3e, respectively). The DDA results revealed that the E-field was enhanced near the bumpy AgNS surface across all wavelengths and that its distribution was gradually increased as the wavelength of incident light varied from the visible to the NIR region. In addition, a highly localized E-field at the tips of the bumpy AgNS surface was shown under the NIR incident light (785 nm), which was 2.6 times larger than the value under visible incident light (532 nm). These simulation results demonstrate that AgNS can generate very strong SERS signals at the NIR excitation region.

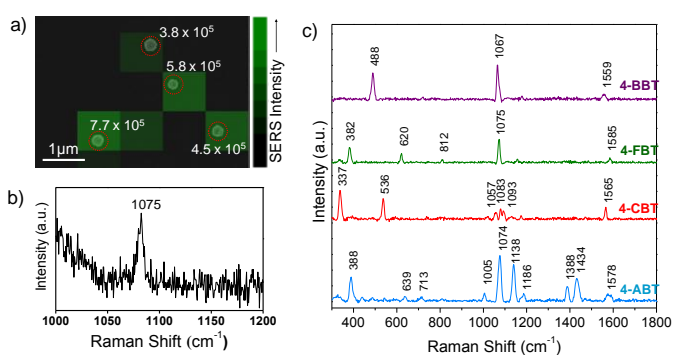


Fig. 4 Signal sensitivity and multiplex capacity of bumpy AgNS based NIR-SERS probes. a) SERS intensity map with enhancement factor values of single AgNS particle bearing 4-FBT; the intensity map was overlaid with its corresponding SEM image. b) SERS spectrum obtained from a single AgNS particle bearing 4-FBT. c) SERS spectra of simple aromatic compounds such as 4-bromobenzenethiol (4-BBT), 4-FBT, 4-chlorobenzenethiol (4-CBT), and 4-aminobenzenethiol (4-ABT) on bumpy AgNS.

Furthermore, we performed SERS measurement on a single AgNS particle in the NIR window as previously reported. 15 Briefly, after the AgNS suspension was drop-cast on a patterned silicon wafer, SERS was measured using point-bypoint mapping with a step size of 1 µm, an integration time of 10 s, and a 785-nm photo-excitation of 28-µW laser power. The same area of Raman mapping was then imaged with SEM to correlate the Raman map and SEM image to ensure single particles. Fig. 4a shows the overlaid image of the SERS intensity map with the SEM image of single AgNS particles, indicating that SERS mapping exactly corresponds to the position of each single particle. In addition, Fig. 4b shows a typical spectrum obtained from single particle SERS measurement. Figs. 4a and 4b demonstrate that the SERS signals of 4-FBT adsorbed on single AgNS particles is strong enough to be detected in the NIR window (average SERS enhancement factor is 6.4 ×10⁵). Such highly sensitive SERS effect can be attributed to the bumpy structure of AgNS that has four times stronger E-field enhancement than that of the smooth AgNS or AuNS (see ESI Fig. S6†). According to the results obtained so far, bumpy AgNS-10 with a thickness of 39 nm is the most suitable NIR-active SERS substrate for sensitive detection and bio-imaging. We then prepared four types of SERS nanoprobes by introducing different RLCs including 4bromobenzenethiol (4-BBT), 4-FBT, 4-chlorobenzenethiol (4-CBT), and 4-aminobenzenethiol (4-ABT) on bumpy AgNS,

Journal Name COMMUNICATION

which are denoted AgNS[4BBT], AgNS[4FBT], AgNS[4CBT], and $AgNS_{\rm [4ABT]},$ respectively. Each $AgNS_{\rm [RLC]}$ has its own SERS spectrum without overlapping with the others (Fig. 4c), and thus can be used as a unique barcode in the multiplexed detection of various target molecules.

To improve the biocompatibility and colloidal stability of SERS NPs, various encapsulation materials such as silica, 2,10,14,15 poly(ethylene glycol) (PEG),5,19,20 and bovine serum albumin (BSA)^{7,21} have been used as a protective layer. In this study, AgNS[RLC] was encapsulated with methoxy poly(ethylene glycol) sulfhydryl (mPEG-SH, MW 5000) (ESI Fig. S7a†). PEG is well known for its ability to prevent NPs from their aggregation and degradation in biological systems and to improve their circulation time in vivo. 19 In order to confirm the effect of PEGylation on the colloidal and signal stability of AgNS_[RLC], the SERS signals of PEGylated AgNS_[4FBT] and non-PEGylated AgNS[4FBT] were obtained. As shown in ESI Fig S7†, no significant change in the SERS intensities was observed from PEGylated AgNS[4FBT] stored at both room temperature and relatively higher temperature (50 °C), suggesting that PEGylated AgNS[4FBT] can exhibit great colloidal stability at human body temperature (~37 °C) for several days. However, the two-fold higher SERS signal was obtained from the non-PEGylated AgNS[4FBT] due to its aggregation, creating "SERS hot spots" after 1 day incubation at 50 °C. The surface morphology of all the AgNS[4FBT] remained the same after a stability test for a certain period of time according to TEM analysis (ESI Fig. S9†). Hence, we conclude that the PEGylated AgNS is suitable to be used as SERS nanoprobes for a long-term SERS detection in vivo.

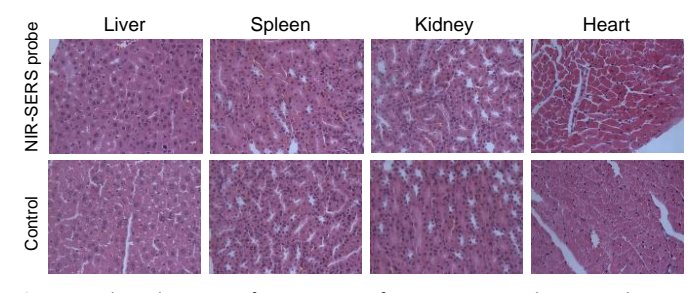


Fig. 5 Histological staining of major organs from NIR-SERS probes-treated mice. H&E stained slices for liver, spleen, kidney, and heart (left to right). The top row shows tissues from NIR-SERS probe treated mice. The bottom row shows tissues from control mice. No significant differences were observed between the NIR-SERS probe treated mice and the control mice specimens.

To investigate the *in vivo* toxicity of the PEGylated AgNS_[4FBT] (denoted as NIR-SERS probe[4FBT]), we conducted a liver function test and hematologic and histologic evaluation after a tail vein injection of the NIR-SERS probe[4FBT] (dose=50 mg kg-1; based on Ag weight) to a live mouse. All mice were sacrificed at the same time, 3 days after the injection of the NIR-SERS probe. As shown in ESI Fig. S10†, SERS signals of the NIR-SERS probe[4FBT] were detected from the major organs such as the liver and spleen where NPs are normally accumulated. 42 Hematologic evaluation results showed that the levels of hematological markers, white blood cells, hemoglobin, and platelets were not significantly changed in the NIR-SERS probe treated mice compared with the control group (ESI Table S2†). In addition, no significant differences in the levels of alkaline phosphate (ALP), alanine aminotransferase (ALT), total bilirubin, albumin, cholesterol, and γ-glutamyl transferase (GGT) (ESI Table S3†) were observed. No tissue damage, inflammation, or morphological change was found in any of the

organs examined (liver, spleen, kidney, and heart), and no significant difference in histologic evaluation was found between the NIR-SERS probe treated mice and the control mice (Fig. 5). These results indicate that the testing dose of the NIR-SERS probe (< 50 mg kg⁻¹) did not cause any in vivo toxicity, which is a critical feature for further biomedical applications. Finally, NIR-SERS probes were applied to cell-tracking in a xenograft mouse model. After internalization of the NIR-SERS probes[4FBT] into adenocarcinomic human alveolar basal epithelial cells (A549 cells), the A549 cell suspension was subcutaneously injected into a nude mouse (ESI Fig. S7b†). First, we confirmed whether or not the NIR-SERS probes[4FBT] were successfully internalized into the A549 cells by using a confocal micro-Raman system before cell-tracking in vivo.

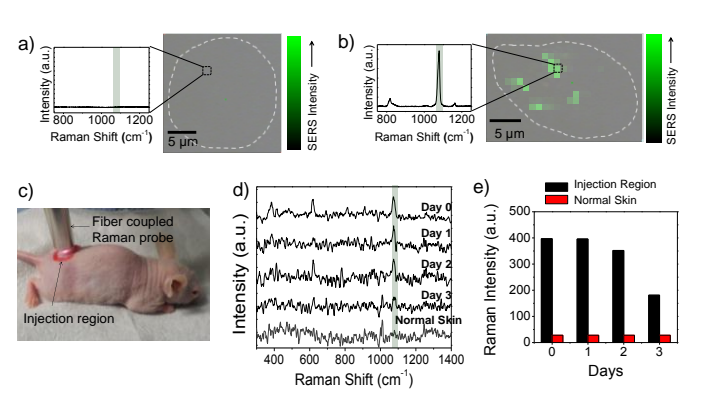


Fig. 6 In vivo cell tracking using NIR-SERS probes. a) SERS intensity map of A549 cell without treatment of NIR-SERS probes $_{[4FBT]}$ and b) with treatment of NIR-SERS probes[4FBT]. The SERS intensity map was overlaid with the optical image of the cell. White dotted lines indicate a cell boundary. The 785 nm photoexcitation of 31 mW laser power and light acquisition time of 1 s. c) A photograph showing the area of a mouse where the A549 cells containing NIR-SERS probes[4FBT] were injected, and an optical fibre coupled Raman probe. d) SERS spectra of NIR-SERS probes[4FBT] obtained from a mouse as a function of time after injection periods from 0 to 3 days with the 785 nm photo-excitation of 90 mW laser power and light acquisition time of 30 s. e) SERS intensities of the NIR-SERS probe[4FBT] peaks appearing at 1075 cm⁻¹ in the spectra shown in (d).

As shown in Figs. 6a and 6b, the intense SERS signal of the NIR-SERS probe[4FBT] was observed from the A549 cells after incubation with the NIR-SERS probes[4FBT] while there was no SERS signal from the cells without treatment of NIR-SERS probes. This result indicates that NIR-SERS probes can be internalized into A549 cells via natural endocytosis. In addition, the NIR-SERS probe[4FBT] showed no significant cytotoxicity in A549 cells up to a 0.1 nM (100 µL) concentration as shown in ESI Fig. S11†. After the subcutaneous injection of the A549 cells (100 μ L, 6 \times 10⁵ mL⁻¹) containing the NIR-SERS probes[4FBT] into a gluteal region of a nude mouse, the SERS spectra were measured from the injected region using an optical fiber coupled portable Raman with 785 nm photo-excitation (Fig. 6c). As shown in Figs. 6d and 6e, the intense SERS signals (1075 cm⁻¹) of the NIR-SERS probe[4FBT] were observed from the injected area of the mouse immediately after cell injection. In addition, the SERS signal remained intense for two days after injection. However, the SERS intensity of the peak at 1075 cm⁻¹ decreased after three days. We speculate that this diminution of the SERS signal could be caused by cell division that leads to the dilution of the NIR-SERS probe[4FBT] inside the cells as previously reported.⁴³ This result demonstrates that NIR-SERS probes based on bumpy AgNS were successfully

Journal Name

applied to cell tracking in living animals using a portable Raman system.

In summary, we have developed NIR active, ultrasensitive, and biocompatible SERS probes based on AgNS with bump-structures by using the seedless one-step deposition method. The NIR SERS activities of bumpy AgNS were tuned by adjusting the thickness of the silver shell (ca. 32-76 nm). They exhibited strong Raman signals at the single-particle detection level, which had originated from highly enhanced E-field at the tips of bumps on the AgNS surface. In addition, the NIR-SERS probes exhibited high colloidal stability and no significant in vivo toxicity applicable for long-term in vivo cell tracking. The A549 cells labeled with NIR-SERS probes[4FBT] were subcutaneously injected into a nude mouse and successfully tracked in vivo for three days. The bumpy AgNS based NIR-SERS probe is an ultrasensitive nanoprobe the potential application of which can be considered in diagnostic platform development, in vivo high throughput screening of bio-ligand, and image-guided therapy.

Acknowledgements

This research was supported by the Pioneer Research Centre Program (NRF-2011-0027888) and the Basic Science Research Program (Grant Number 2012-R1A1A1012516) through the National Research Foundation of Korea funded by the Ministry of Science, ICT & Future Planning.

Notes and references

- ^a Interdisciplinary Program in Nano-Science and Technology, Seoul National University, Seoul, 151-742, Republic of Korea.
- b School of Chemical and Biological Engineering, Seoul National University, Seoul, 151-742, Republic of Korea.
- ^c Laboratory of Toxicology, College and Veterinary Medicine, Seoul National University, Seoul 151-742, Republic of Korea.
- ^d Program in Nano Science and Technology, Graduate School of Convergence Science and Technology, Seoul National University, Seoul 151-742, Republic of Korea.
- ^e Medical Supplies Evaluation Center, Korea Testing Certification, Gunpo, 435-862, Republic of Korea.
- Jepartment of Nuclear Medicine, Seoul National University Bundang Hospital, Seongnam, 463-707, Republic of Korea.
- g Department of Chemistry Education, Seoul National University, Seoul, 151-742, Republic of Korea.
- ^h Graduate Group of Tumor Biology, Seoul National University, Seoul 151-742, Republic of Korea.
- ¹ Department of Chemical Engineering, Hanyang University, Ansan 426-791, Republic of Korea.
- ^j Advanced Institute of Convergence Technology, Seoul National University, Suwon 443-270, Republic of Korea.
- * To whom correspondence should be addressed.
- E-mail: debobkr@gmail.com (H.Y Lee), kjh75@hanyang.ac.kr (J. H. Kim), jeongdh@snu.ac.kr (D.H. Jeong), yslee@snu.ac.kr (Y. S. Lee).
- † Electronic Supplementary Information (ESI) available: Experimental section, cyclic voltammograms, electron microscope images, and toxicity data. See DOI: 10.1039/c000000x/
- ‡ Current address: School of Electrical Engineering and Computer Science, Seoul National University, Seoul 151-742, Republic of Korea.
- D. Graham, W. E. Smith, A. M. Linacre, C. H. Munro, N. D. Watson and P. C. White, *Anal. Chem.*, 1997, **69**, 4703-4707; J. Ni, R. J. Lipert, G. B. Dawson and M. D. Porter, *Anal. Chem.*, 1999, **71**, 4903-4908; G. L. Liu, Y. Lu, J. Kim, J. C. Doll and L. P. Lee, *Adv. Mater.*, 2005, **17**, 2683-2688; J. Kneipp, H. Kneipp, M. McLaughlin, D. Brown and K. Kneipp,

- Nano Lett., 2006, 6, 2225-2231; H. Chon, S. Lee, S. W. Son, C. H. Oh and J. Choo, Anal. Chem., 2009, 81, 3029-3034.
- S. P. Mulvaney, M. D. Musick, C. D. Keating and M. J. Natan, *Langmuir*, 2003, 19, 4784-4790; W. E. Doering and S. Nie, *Anal. Chem.*, 2003, 75, 6171-6176.
- C. L. Zavaleta, B. R. Smith, I. Walton, W. Doering, G. Davis, B. Shojaei, M. J. Natan and S. S. Gambhir, *Proc. Natl. Acad. Sci. U. S. A.*, 2009, 106, 13511-13516.
- S. Nie and S. R. Emory, *Science*, 1997, 275, 1102; K. Kneipp, Y. Wang, H. Kneipp, L. T. Perelman, I. Itzkan, R. R. Dasari and M. S. Feld, *Phys. Rev. Lett.*, 1997, 78, 1667-1670; D. K. Lim, K. S. Jeon, H. M. Kim, J. M. Nam and Y. D. Suh, *Nat. Mater.*, 2010, 9, 60-67.
- 5. L. Sun, C. Yu and J. Irudayaraj, Anal. Chem., 2007, 79, 3981-3988.
- J. H. Kim, H. Kang, S. Kim, B. H. Jun, T. Kang, J. Chae, S. Jeong, J. Kim, D. H. Jeong and Y. S. Lee, *Chem. Commun.*, 2011, 47, 2306-2308;
 Y. W. C. Cao, R. Jin and C. A. Mirkin, *Science*, 2002, 297, 1536-1540;
 M. Moskovits, *Rev. Mod. Phys.*, 1985, 57, 783-826.
- H. Yuan, Y. Liu, A. M. Fales, Y. L. Li, J. Liu and T. Vo-Dinh, *Anal. Chem.*, 2013, 85, 208-212.
- B.-H. Jun, M. S. Noh, G. Kim, H. Kang, J.-H. Kim, W.-J. Chung, M.-S. Kim, Y.-K. Kim, M.-H. Cho, D. H. Jeong and Y.-S. Lee, *Anal. Biochem.*, 2009, 391, 24-30; S. Schlücker, *ChemPhysChem*, 2009, 10, 1344-1354.
- R. A. Alvarez-Puebla, D. J. Ross, G. A. Nazri and R. F. Aroca, *Langmuir*, 2005, 21, 10504-10508.
- B. Küstner, M. Gellner, M. Schütz, F. Schöppler, A. Marx, P. Ströbel, P. Adam, C. Schmuck and S. Schlücker, *Angew. Chem. Int. Ed.*, 2009, 48, 1950-1953.
- C. E. Talley, J. B. Jackson, C. Oubre, N. K. Grady, C. W. Hollars, S. M. Lane, T. R. Huser, P. Nordlander and N. J. Halas, *Nano Lett.*, 2005, 5, 1569-1574.
- Y. Zhang, J. Qian, D. Wang, Y. Wang and S. He, *Angew. Chem. Int. Ed.*, 2013, 52, 1148-1151; J. V. Jokerst, A. J. Cole, D. Van de Sompel and S. S. Gambhir, *ACS Nano*, 2012, 6, 10366-10377.
- L. Rodríguez-Lorenzo, Z. Krpetic, S. Barbosa, R. A. Alvarez-Puebla, L. M. Liz-Marzán, I. A. Prior and M. Brust, *Integrative Biology*, 2011, 3, 922-926.
- 14. J. H. Kim, J. S. Kim, H. Choi, S. M. Lee, B. H. Jun, K. N. Yu, E. Kuk, Y. K. Kim, D. H. Jeong, M. H. Cho and Y. S. Lee, *Anal. Chem.*, 2006, 78, 6967-6973.
- H. Kang, S. Jeong, Y. Park, J. Yim, B.-H. Jun, S. Kyeong, J.-K. Yang, G. Kim, S. Hong, L. P. Lee, J.-H. Kim, H.-Y. Lee, D. H. Jeong and Y.-S. Lee, Adv. Funct. Mater., 2013, 23, 3719–3727.
- X. Su, J. Zhang, L. Sun, T.-W. Koo, S. Chan, N. Sundararajan, M. Yamakawa and A. A. Berlin, *Nano Lett.*, 2005, 5, 49-54; P. J. Huang, L. K. Chau, T. S. Yang, L. L. Tay and T. T. Lin, *Adv. Funct. Mater.*, 2009, 19, 242-248; M. Gellner, D. Steinigeweg, S. Ichilmann, M. Salehi, M. Schütz, K. Kömpe, M. Haase and S. Schlücker, *Small*, 2011, 7, 3445-3451; J. H. Yoon, J. Lim and S. Yoon, *ACS Nano*, 2012, 6, 7199-7208.
- S. Pande, S. K. Ghosh, S. Praharaj, S. Panigrahi, S. Basu, S. Jana, A. Pal, T. Tsukuda and T. Pal, *J. Phys. Chem. C*, 2007, **111**, 10806-10813.
- R. Weissleder, Nat. Biotechnol., 2001, 19, 316-317; Y. Wang, J. L. Seebald, D. P. Szeto and J. Irudayaraj, ACS Nano, 2010, 4, 4039-4053;
 M. V. Yigit, L. Zhu, M. A. Ifediba, Y. Zhang, K. Carr, A. Moore and Z. Medarova, ACS Nano, 2011, 5, 1056-1066; K. K. Maiti, U. S. Dinish, A. Samanta, M. Vendrell, K. S. Soh, S. J. Park, M. Olivo and Y. T. Chang, Nano Today, 2012, 7, 85-93; H. n. Xie, R. Stevenson, N. Stone, A. Hernandez Santana, K. Faulds and D. Graham, Angew. Chem. Int. Ed., 2012, 51, 8509-8511.
- X. Qian, X. H. Peng, D. O. Ansari, Q. Yin-Goen, G. Z. Chen, D. M. Shin, L. Yang, A. N. Young, M. D. Wang and S. M. Nie, *Nat. Biotechnol.*, 2008, 26, 83-90; J. Qian, L. Jiang, F. Cai, D. Wang and S. He, *Biomaterials*, 2011, 32, 1601-1610.

 G. von Maltzahn, A. Centrone, J. H. Park, R. Ramanathan, M. J. Sailor, T. A. Hatton and S. N. Bhatia, Adv. Mater., 2009, 21, 3175-3180.

Journal Name

- A. Samanta, K. K. Maiti, K. S. Soh, X. Liao, M. Vendrell, U. S. Dinish, S. W. Yun, R. Bhuvaneswari, H. Kim, S. Rautela, J. Chung, M. Olivo and Y. T. Chang, *Angew. Chem. Int. Ed.*, 2011, 50, 6089-6092.
- S. Oldenburg, R. Averitt, S. Westcott and N. Halas, *Chem. Phys. Lett.*, 1998, 288, 243-247; M. Gellner, B. Küstner and S. Schlücker, *Vib. Spectrosc.*, 2009, 50, 43-47.
- 23. J. Jackson and N. Halas, J. Phys. Chem. B, 2001, 105, 2743-2746.
- J. B. Jackson and N. J. Halas, Proc. Natl. Acad. Sci., 2004, 101, 17930-17935.
- K. Kneipp, H. Kneipp and J. Kneipp, Acc. Chem. Res., 2006, 39, 443-450; K. Kneipp, R. R. Dasari and Y. Wang, Appl. Spectrosc., 1994, 48, 951-955; J. Choo and H. Chon, in Optical Spectroscopy and Computational Methods in Biology and Medicine, ed. M. Baranska, Springer Netherlands, 2014, vol. 14, pp. 401-417.
- J.-H. Kim, W. W. Bryan and T. Randall Lee, *Langmuir*, 2008, 24, 11147-11152.
- A. Dong, Y. Wang, Y. Tang, N. Ren, W. Yang and Z. Gao, *Chem. Commun.*, 2002, 350-351.
- 28. Z. Liang, A. S. Susha and F. Caruso, Adv. Mater., 2002, 14, 1160.
- 29. Q. Wu, C. Zhang and F. Li, Mater. Lett., 2005, 59, 3672-3677.
- K.-T. Yong, Y. Sahoo, M. T. Swihart and P. N. Prasad, *Colloids Surf.*, A, 2006, 290, 89-105; S. Long, L. Li, H. Guo, W. Yang and F. Lu, *Dyes Pigm.*, 2012; C. Zhang, X. Zhu, H. Li, I. Khan, M. Imran, L. Wang, J. Bao and X. Cheng, *Nanoscale Res. Lett.*, 2012, 7, 1-7; T. Liu, D. Li, D. Yang and M. Jiang, *Colloids Surf.*, A, 2011, 387, 17-22; J. Zhang, H. Liu, Z. Wang and N. Ming, *Mater. Lett.*, 2007, 61, 4579-4582.
- 31. Z.-j. Jiang and C.-y. Liu, J. Phys. Chem. B, 2003, 107, 12411-12415.
- J. Zhang, J. Liu, S. Wang, P. Zhan, Z. Wang and N. Ming, Adv. Funct. Mater., 2004, 14, 1089-1096; L. Chen, X. Han, J. Yang, J. Zhou, W. Song, B. Zhao, W. Xu and Y. Ozaki, J. Colloid Interface Sci., 2011, 360, 482-487.
- 33. V. G. Pol, D. Srivastava, O. Palchik, V. Palchik, M. Slifkin, A. Weiss and A. Gedanken, *Langmuir*, 2002, **18**, 3352-3357; S. Tang, Y. Tang, S. Zhu, H. Lu and X. Meng, *J. Solid State Chem.*, 2007, **180**, 2871-2876; X. Ye, Y. Zhou, J. Chen and Y. Sun, *Appl. Surf. Sci.*, 2007, **253**, 6264-6267.
- S. Kalele, S. Ashtaputre, N. Hebalkar, S. Gosavi, D. Deobagkar, D. Deobagkar and S. Kulkarni, *Chem. Phys. Lett.*, 2005, 404, 136-141.
- C. Tian, E. Wang, Z. Kang, B. Mao, C. Zhang, Y. Lan, C. Wang and Y. Song, J. Solid State Chem., 2006, 179, 3270-3276; J. C. Flores, V. Torres, M. Popa, D. Crespo and J. M. Calderón-Moreno, Colloids Surf., A, 2008, 330, 86-90.
- H. Wang, G. P. Goodrich, F. Tam, C. Oubre, P. Nordlander and N. J. Halas, J. Phys. Chem. B, 2005, 109, 11083-11087.
- 37. J. Newman and G. Blanchard, Langmuir, 2006, 22, 5882-5887.
- K. Naka and Y. Chujo, in *Nanohybridization of Organic-Inorganic Materials*, Springer, 2009, pp. 3-40.
- B. H. Jun, G. Kim, J. Baek, H. Kang, T. Kim, T. Hyeon, D. H. Jeong and Y. S. Lee, *Phys. Chem. Chem. Phys.*, 2011, 13, 7298-7303; H. Kang, T. Kang, S. Kim, J. H. Kim, B. H. Jun, J. Chae, J. Park, D. H. Jeong and Y. S. Lee, *J. Nanosci. Nanotechnol.*, 2011, 11, 579-583.
- M. J. Carter, D. P. Rillema and F. Basolo, J. Am. Chem. Soc., 1974, 96, 392-400; U. Sivagnanam and M. Palaniandavar, J. Chem. Soc., Dalton Trans., 1994, 2277-2283.
- H. Wang, K. Fu, R. Drezek and N. Halas, Appl. Phys. B, 2006, 84, 191-195.
- D. K. Tiwari, T. Jin and J. Behari, *Toxicol. Mech. Methods*, 2011, 21, 13-24.
- 43. B.-H. Jun, D. W. Hwang, H. S. Jung, J. Jang, H. Kim, H. Kang, T. Kang, S. Kyeong, H. Lee, D. H. Jeong, K. W. Kang, H. Youn, D. S. Lee and Y.-S. Lee, *Adv. Funct. Mater.*, 2012, 22, 1843-1849.

Graphical Astract

Title: One-Step Synthesis of Silver Nanoshell with Bumps for
Highly Sensitive Near-IR SERS Nanoprobes

Based on AgNS with bump-structures, the NIR active, ultrasensitive, and biocompatible SERS probes were developed and applied for *in vivo* cell tracking in a live animal.

